

# A Forming Wide Polar Ring Galaxy at $z \sim 0.05$ in the VST Deep Field of the Fornax Cluster<sup>\*</sup>

E. Iodice<sup>1</sup>, M. Capaccioli<sup>1,2</sup>, M. Spavone<sup>1</sup>, N.R. Napolitano<sup>1</sup>, A. Grado<sup>1</sup>, L. Limatola<sup>1</sup>, M. Cantiello<sup>3</sup>, and P. Schipani<sup>1</sup>

<sup>1</sup> INAF-Osservatorio Astronomico di Capodimonte, via Moiariello 16, I-80131 Naples, Italy e-mail: iodice@na.astro.it

<sup>2</sup> Dipartimento di Fisica, Università di Napoli "Federico II", via Cintia 21, I-80126 Naples, Italy

<sup>3</sup> INAF - Osservatorio Astronomico di Teramo, via Maggini, I-64100 Teramo, Italy

Received ....; accepted ...

## ABSTRACT

We present the first deep photometry of a good candidate for a forming polar ring galaxy at redshift  $z \approx 0.05$ . This object, named FCSS J033710.0-354727, is a background galaxy in the VST deep field of the Fornax cluster. The deep exposures combined with the high angular resolution of the OmegaCAM at VST allow us to carry out the first detailed photometric analysis for this system in the  $g$  and  $i$  bands to derive the galaxy structure and colors. Results show that the central object resembles a disk galaxy, surrounded by a ring-like structure 2 times more extended than the central disk. The warped geometry and the presence of bright knots observed along the polar direction, as well as the several debris detected on the NW side with colors comparable to those of the galaxy, suggest that the polar structure is still forming. We argue that the wide polar ring/disk is the result of the ongoing disruption of a companion galaxy in the potential of the central object, which is 2-3 times more massive than the accreting galaxy.

**Key words.** Galaxies: photometry; peculiar; structure; formation - Astronomical data bases: Surveys

## 1. Introduction

Polar Ring/Disk Galaxies (PRGs) are multi-spin systems. The polar structure is made by dust and gas that rotates in a perpendicular plane with respect to the stars of the central galaxy (see Iodice 2014, as a review). A "second event" is invoked in the formation history of PRGs in order to explain the decoupling of the angular momentum. Thus, PRGs are among the best galaxies to study the physics of accretion/interaction mechanisms, the disk formation and the dark halo shape. New deep surveys have shown that multi-spin galaxies are quite common at high redshift and studying these systems at increasing redshift gives fundamental information on the physical processes at work (i.e. merging and accretion) during the formation of galaxies (see Conselice 2014, as a review). In the literature there are few studies on PRGs at high redshifts ( $z \geq 0.05$ ), where the dominant component, the central galaxy, is easily visible, while detection of the faint, bluer and dusty polar structure requires deep imaging, with high spatial resolution. The most distant kinematically confirmed PRG is at  $z \sim 0.06$  (Brosch et al. 2010). At higher redshifts ( $z \sim 0.06 - 1.3$ ), there are only few PRG candidates to be confirmed (Reshetnikov 1997; Reshetnikov & Dettmar 2007). The photometric analysis performed on PRGs at  $z \geq 0.05$  shows that in all of them the polar structure has an almost regular ring-like shape, with some clumps of light due to star forming regions. Up to date there is not a detailed study of a *forming* PRG, where the polar structure is still ongoing in an intermediate stage, like the well studied galaxies NGC 3808B and NGC6286 at  $z \sim 0.02$  (Reshetnikov et al. 1996). In the new SDSS-based Polar Ring Catalogue (SPRC) compiled by Moiseev et al. (2011), which reports several new PRG candidates in

a large range of redshift, only two objects resemble an ongoing interaction to form a PRG at  $z \geq 0.05$  (SPRC199 and SPRC226), but both of them are neither kinematically confirmed nor studied in detail. At  $z \sim 0.02$  a forming polar disk is found in the wall between voids, resulting from the slow accretion of gas (Stanonik et al. 2009): the polar structure is made only by neutral hydrogen (it was detected in the HI emission) and the gas density is still too low to form the stellar counterpart. In this letter we present the detailed photometric analysis of the background galaxy FCSS J033710.0-354727 at  $z \sim 0.05$ , which is a good candidate to be the first forming wide PRG at this redshift.

## 2. Observations and Data Reduction

As part of the *VST Survey of Elliptical Galaxies in the Southern hemisphere* (VEGAS Capaccioli & Schipani 2011, see), which is a Guaranteed Time Observation survey being performed at the ESO VLT Survey Telescope (VST), we have obtained a mosaic of  $1.75 \times 1.59$  degree of the Deep Field of the Fornax Cluster, around the cD galaxy NGC 1399. Images are collected in the  $g$  and  $i$  bands, on October 2011. VST is a 2.6-m wide field optical survey telescope, located at Cerro Paranal in Chile. The VST is currently the largest telescope in the world specially designed for surveying the sky in visible light; it is the ESO work-horse totally dedicated to visible survey programmes. The telescope is a F/5.5 with an alt-azimuth mount, equipped with an active optics system (Schipani et al. 2010, 2012). VST is equipped with the wide field camera OmegaCAM, spanning a  $1 \times 1$  degree<sup>2</sup> field of view, in the optical wavelength range from 0.3 to 1.0 micron (Kuijken 2011). The mean pixel scale is 0.21 arcsec/pixel. The region of maximum overlap of all pointings is around the galaxy NGC 1389, where the total integration time is 3 hours in the  $g$

<sup>\*</sup> This work is based on observations taken at the ESO La Silla Paranal Observatory within the VST GTO Program ID 088.B-4012(A).

band and 1.4 hours in the  $i$  band. The average seeing is about 1 arcsec.

The data reduction has been performed with the *VST-Tube* imaging pipeline (Grado et al. 2012). From the raw data, it provides fully calibrated images, throughout the following steps: 1) overscan, bias and flat-field correction; 2) CCD gain equalization and illumination correction; 3) astrometric and photometric calibration, applied before stacking for the final co-added image. For a detailed description of the data reduction procedure see Ripepi et al. (2014). In order to perform a deep surface photometry of the extended galaxies in the VEGAS Survey, the VST-Tube pipeline also includes a task to remove the background patterns. This will be described in the forthcoming paper, which is dedicated to the first results of the VEGAS Survey (Capaccioli et al. in preparation). In the present work, since the studied object covers a very small area (its diameter is  $D \lesssim 30$  arcsec, see Sec. 3), the background has been estimated locally, in the regions surrounding the galaxy.

### 3. The Galaxy FCSS J033710.0-354727: morphology and light distribution

The background galaxy FCSS J033710.0-354727 at  $z \sim 0.051$ , is located South of the bright S0 galaxy NGC 1389 in the Fornax cluster (see Fig. 1). It is characterized by a central component, that we named "host galaxy" (HG), surrounded by a warped ring-like structure (see left panel of Fig. 2 and Fig. 3). The main properties of FCSS J033710.0-354727 are listed in Table 1. According to Brocca et al. (1997), inside a distance of about five times its diameter, i.e.  $R \leq 200$  kpc (see Table 1), no companion galaxies at comparable measured redshift are found around FCSS J033710.0-354727, which could be an isolated object. We have analysed images in the  $g$  and  $i$  bands to derive the galaxy structure and colors.

*Morphology* - The VST image of FCSS J033710.0-354727 in  $g$  and  $i$  bands are shown in the left panels of Fig. 2 and Fig. 3. The center of the galaxy, labelled as **X**, contributes for the most of the light. Towards the North, there are two other bright knots, labelled as **Y** and **Z**, which are inside the polar structure. At larger distances from the galaxy center, we observe several bright features, which are apparently distributed on elliptical orbit around the polar direction, one of this (labelled as **A**) is likely a disk galaxy. None of the above objects have a redshift measurement. We have derived the *high frequency residual images* of FCSS J033710.0-354727 in the  $g$  and  $i$  bands (see right panels of Fig. 2 and Fig. 3), as the ratio of the original reduced image with a smoothed<sup>1</sup> one, where each original pixel value is replaced with the median value in a rectangular window. The *high frequency residual images* shows a disk-like structure along the major axis of the central component. The polar structure extends up to the galaxy center, crossing it by tracing an "S-shaped" pattern. It is characterized by a very bright peak at the end of the North arm. In Fig. 4 it is shown the  $g$  band image of FCSS J033710.0-354727 with different contrast: close to center, the light of the HG is not symmetric and it is perturbed by the two arms of the polar structure that are approaching the nucleus. In particular, on the NE side there is a third bright knot, which light is smeared in the light coming from the central HG. Even if the morphology of FCSS J033710.0-354727 could be also similar to that of late-type barred galaxy (where the central disk could be the bar with loosely wound and highly-inclined arms), the qualitative

<sup>1</sup> We used the IRAF task FMEDIAN to smooth the original reduced image, by adopting a box of  $25 \times 25$  pixels.

**Table 1.** Global properties of FCSS J033710.0-354727.

Parameter	Value	Ref.
Morphological type	Sc peculiar	NED <sup>a</sup>
R.A. (J2000)	03h37m09.94s	NED
Decl. (J2000)	-35d47m27.2s	NED
Helio. radial velocity	15447 km/s	NED
Redshift	0.051	FCSS <sup>b</sup>
Distance	206 Mpc	
scale	1 kpc/arcsec	
Diameters	$3.4 \times 40$ kpc	this work
Magnitudes <sup>c</sup>		this work
$m_g$	18.59 mag	
$m_i$	18.03 mag	
$M_g$	-18.00 mag	
$M_i$	-18.48 mag	
	<i>Central galaxy:</i>	
$m_g$	20.47 mag	
$m_i$	19.90 mag	
$M_g$	-16.12 mag	
$M_i$	-16.61 mag	
$g - i$	0.6 mag	
	<i>Polar structure:</i>	
$m_g$	19.09 mag	
$m_i$	18.53 mag	
$M_g$	-17.54 mag	
$M_i$	-17.99 mag	
$g - i$	0.56 mag	

<sup>a</sup> NASA/IPAC Extragalactic Database

<sup>b</sup> *The Fornax Spectroscopic Survey* (Drinkwater et al. 2000)

<sup>c</sup> Absolute magnitudes are corrected for both Galactic Extinction and K-correction, while apparent magnitudes take into account only the Galactic Extinction, see text for details.

analysis of the structure observed for FCSS J033710.0-354727 described above suggests to classify this object as PRG. In fact, the two arms of the polar structure cross the center of the galaxy, they do not start from the edge of the central disk/bar. Moreover, the "accreting loop" observed towards the galaxy center was also observed in other forming polar rings at lower redshifts, such as ESO 474-G26 (see Fig. 14 of Spavone et al. 2012) and VGS31b (see Fig. 4 of Spavone & Iodice 2013).

*Surface photometry* - We used the ELLIPSE task in IRAF on both  $g$  and  $i$  band images to perform the isophotal analysis. All the bright features around FCSS J033710.0-354727, including background objects and bright stars in the field, are masked. The azimuthally averaged surface brightness profiles, the Position Angle (P.A.) and the ellipticity ( $\epsilon$ ) are shown in Fig. 5. The limits of the surface photometry presented in this work are derived as the distance from the center where the galaxy's light blends into the background level, which are found to be 23 arcsec ( $\sim 23$  kpc) in both  $g$  and  $i$  band. The limiting magnitudes corresponding to the limiting radii given above are  $\mu_g = 29.3 \pm 0.3$  mag arcsec<sup>-2</sup> for the  $g$  band, and  $\mu_i = 27.7 \pm 0.3$  mag arcsec<sup>-2</sup> for the  $i$  band. The error estimates on the magnitudes take the uncertainties on the photometric calibration ( $\sim 0.02$  mag) and sky subtraction ( $\approx 0.06$  ADU in the  $g$  band and  $\approx 0.2$  ADU in the  $i$  band) into account.

The azimuthally averaged surface brightness profiles in the  $g$  and  $i$  bands (see Fig. 5, left panel), are quite smooth on the whole range of radii, except for the two peaks of light at  $R \sim 3.5$  arcsec ( $\sim 3.5$  kpc) and  $R \sim 7$  arcsec ( $\sim 7$  kpc), which corresponds

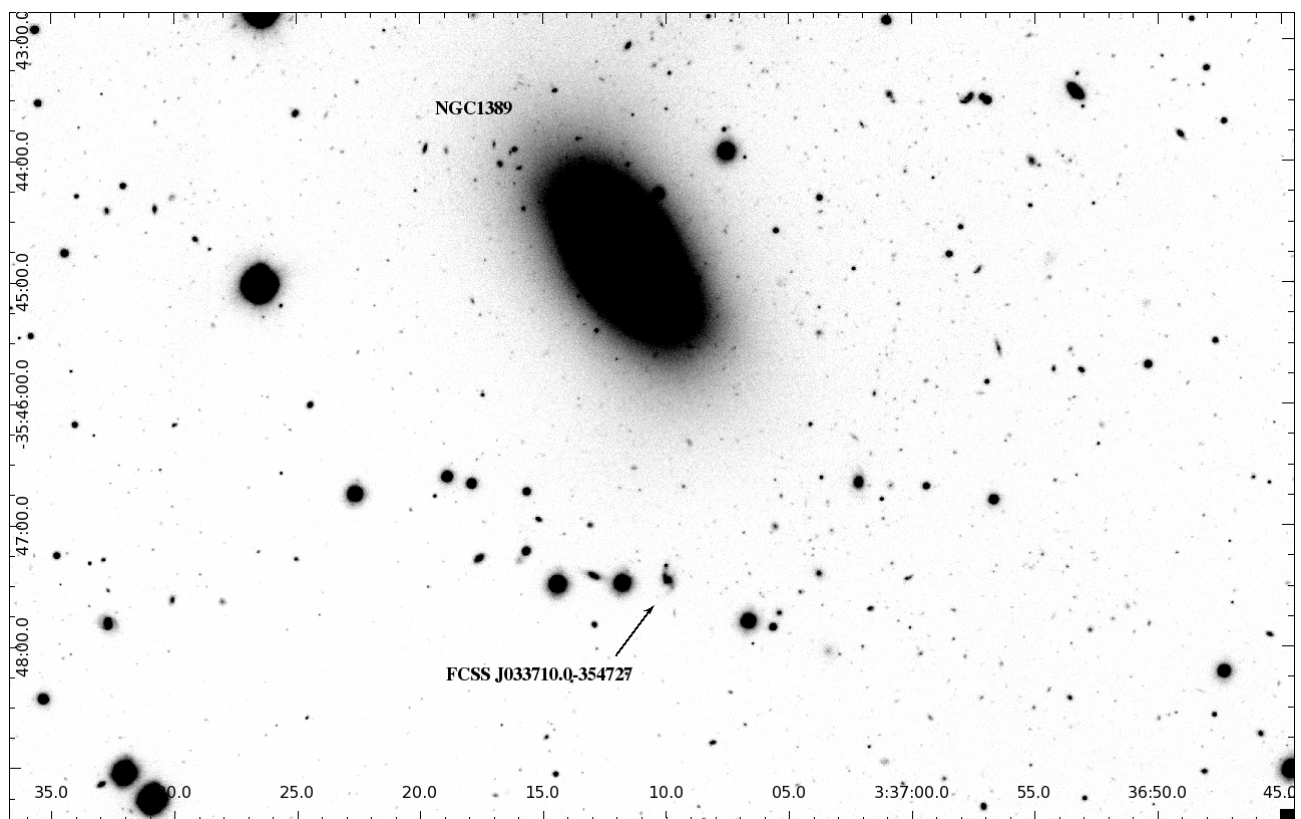


**Fig. 1.** Field around the bright S0 galaxy NGC 1389, in the  $g$ -band VST Deep Field of the Fornax cluster. The arrow locates the background galaxy FCSS J033710.0-354727.

to the bright knots, labeled **Y** and **Z** respectively on Fig. 2 (left panel). Both the P.A. and ellipticity profiles (Fig. 5), show an abrupt change in the shape at  $R \leq 1.69$  arcsec ( $\sim 1.7$  kpc): by looking at the isophotes, in the left panel of Fig. 2, this radius correspond to the "transition" from the HG to polar ring (PR) and set a constraint on the radial extent of the two components, being  $R_{HG} \sim 2$  kpc and  $R_{PR} \sim 20$  kpc. For  $R \geq 1.69$  arcsec, i.e. along the polar structure major axis, and up to  $R \sim 20$  arcsec ( $\sim 1.7 - 20$  kpc), a strong twisting is observed, as the P.A. varies of about  $70^\circ$ . In this range of radii, the flattening increases from 0.1 to 0.4. We obtained the 2-dimensional (2D) model from the fit of the isophotes<sup>2</sup> in the  $g$  band and it has been subtracted off from the original image. The 2D residual is shown in the Fig. 6. As already found from the high-frequency residual image (left panels of Fig. 2 and Fig. 3) and from the high-level contrast in the  $g$  band (see Fig. 4), along the polar direction an "S-shaped" structure is clearly detectable. It extends from the north to the south crossing the galaxy center, drawing a spiral loop throughout the nucleus, and it is characterised by two bright knots in the northern arm.

We derived the integrated magnitudes in the  $g$  and  $i$  bands inside elliptical aperture corresponding to the last fitted isophote for the whole galaxy and for both components (HG and polar structure). Values are corrected for the extinction within the Milky Way, by using the absorption coefficient  $A_g = 0.035$  and  $A_i = 0.018$  derived according to Schlegel et al. (1998). The K-correction was applied to the absolute magnitudes, where the correction factor in  $g$  and  $i$  band are  $K_g = 0.02$  and  $K_i = -0.06$

<sup>2</sup> The 2-dimensional model of the fitted isophotes was obtained by using the IRAF task BMODEL

respectively (Chilingarian et al. 2010; Chilingarian & Zolotukhin 2012).

*Light profiles* - We have extracted the light profiles along the major axis of two main components in FCSS J033710.0-354727 (see Fig. 7). The P.A.s of these directions are defined from the fit of the isophotes (see right panels of Fig. 5). Due to the "S-shape" of the polar structure, which generates the observed twisting, we adopted the two directions at  $P.A. = 8^\circ$  and  $P.A. = 30^\circ$  that intersect the two bright knots **Y** and **Z**.

The surface brightness of the central component extends up to about 8 arcsec ( $\sim 8$  kpc). It is not symmetric with respect to the center of the galaxy. For  $R \geq 2$  arcsec, the NW part of the light profile is brighter than the SE part. We performed a least-square fit of the HG light profiles (NW and SE sides) by using an exponential law given by

$$\mu(R) = \mu_0 + 1.086 \times R/r_h$$

where  $R$  is the galactocentric distance,  $\mu_0$  and  $r_h$  are the central surface brightness and scale length of the disk. The best fit values for the structural parameters found for the NW profile are  $\mu_0^{NW} = 22.21 \pm 0.05$  mag/arcsec<sup>2</sup> and  $r_h^{NW} = 1.89 \pm 0.04$  arcsec and for the SE profile are  $\mu_0^{SE} = 22.07 \pm 0.10$  mag/arcsec<sup>2</sup> and  $r_h^{SE} = 1.41 \pm 0.05$  arcsec. For  $R \leq 2$  arcsec there is an excess of light of about 0.2 mag, which is quite symmetric with respect to the center, contrary to what is observed at larger radii. This feature could be related to a small bulge.

Along the polar structure the surface brightness is twice as extended than that along the HG, out to  $R \sim 20$  arcsec ( $\sim 20$  kpc). The peak of light corresponding to **Z** is less than one magnitude fainter than the galaxy center.

*Integrated magnitudes and colors* - In Fig. 8 it is shown the isophotal  $g - i$  color profile. The central spheroid, for  $R \leq$

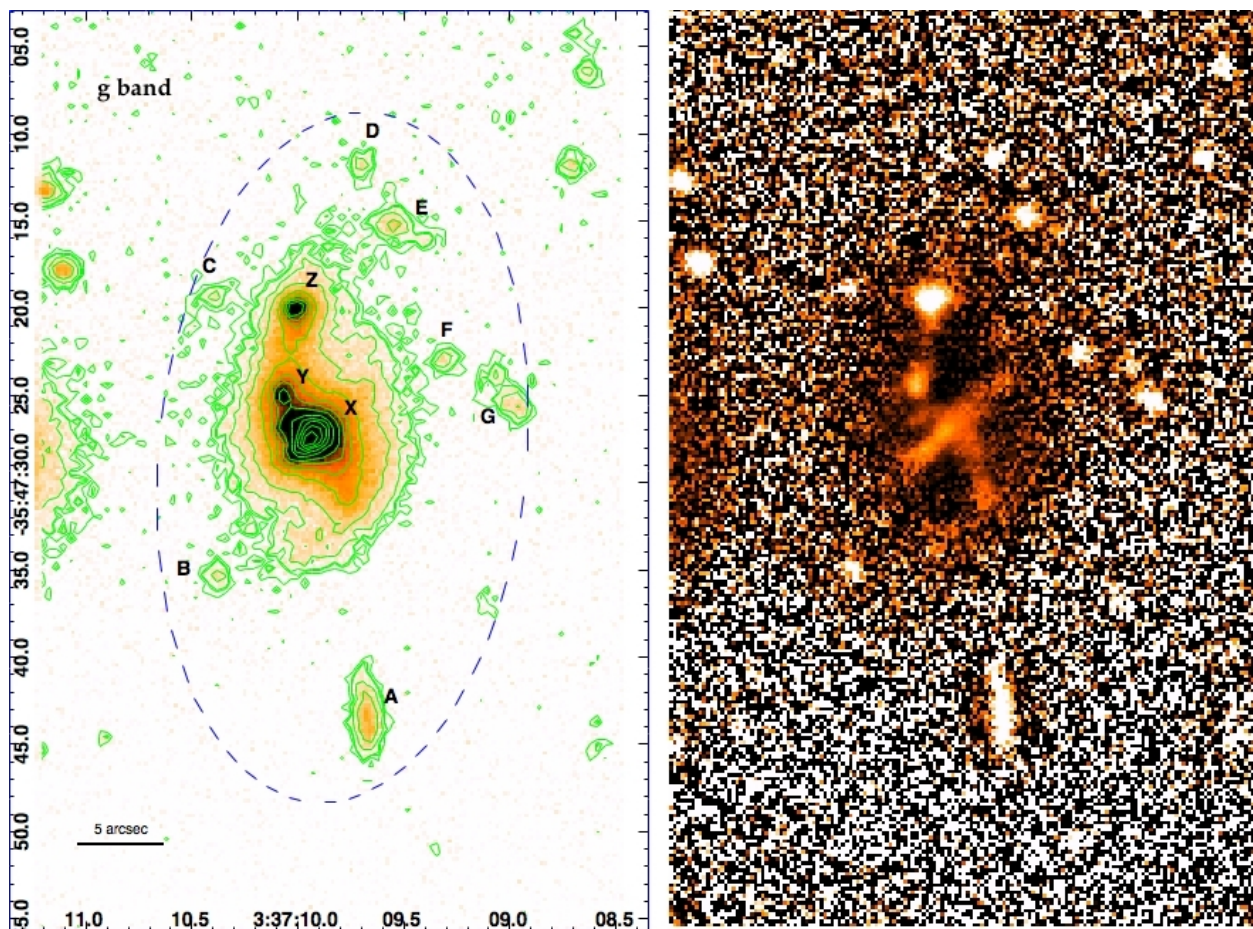


**Fig. 2.** Left panel - VST image of FCSS J033710.0-354727 in  $g$ -band and the isophote contours (green lines). Labels indicate the center of the galaxy, **X**, the two bright knots inside the polar structure, **Y** and **Z**, and several bright features, from **A** to **G** which are apparently distributed on elliptical orbit (blue dashed line) around the polar direction. Right panel - The *high frequency residual images* of FCSS J033710.0-354727 in the  $g$ -band (see Sec. 3 for details). North is up and East is on the left.

1.6 arcsec, is redder than the polar structure, having an average color  $g - i \sim 0.58$  mag. For  $R > 1.6$  arcsec, the color profile has a steep gradient towards bluer colors, reaching a value of  $g - i \sim 0.2$  mag at  $R \sim 10$  arcsec.

We have derived the integrated magnitudes and  $(g - i)$  colors in circular apertures<sup>3</sup> of the center of galaxy, the two bright knots **Y** and **Z**, and of all the bright objects around the galaxy (see left panel of Fig. 2). Values are listed in Table 2. As already shown from the light profiles, the bright knot **Z** on the NE side is only 0.5 magnitude fainter than the galaxy center. The center of the galaxy is redder than the two knots on the North side of the polar structure, and it has  $(g - i) = 0.55$  mag. The closest knot to the central spheroid, labelled as **Y**, has  $(g - i) = 0.35$  mag, while the outer and more luminous knot **Z** of the polar structure has bluer color  $(g - i) = 0.13$  mag. The integrated colors of the bright objects observed around FCSS J033710.0-354727 have a "bimodal" distribution. The galaxy labelled as **A** and the two bright objects **B** and **G** have  $(g - i) \geq 1$  mag, while for all the other sources we measured  $0.3 \leq (g - i) \leq 1$  mag. In particular, the objects **D**, **E** and **F**, located on NW region of FCSS J033710.0-354727, have  $(g - i)$  colors comparable with the range of colors derived for the polar structure. From the  $g - i$  colors, by using the stellar population synthesis model GISSSEL<sup>4</sup> (Bruzual & Char-

lot 2003), we have estimated the mass-to-light ratio ( $M/L$ ) for the central galaxy and the polar structure, in order to constrain the total stellar mass for each component. Assuming a simple stellar population, with a solar metallicity, for the central galaxy the models predict an  $M/L \sim 0.6$  and for the polar structure an  $M/L \sim 0.3-0.6$ . From the total magnitudes in the  $g$  band (see Table 2), the stellar mass in the HG is  $M^{HG} \sim 2 \times 10^8 M_{\odot}$  and in the polar structure is  $M^{PR} \sim 1 \times 10^8 M_{\odot}$ . These should be considered as lower limits for the total baryonic mass, since we do not have any information about the gas content in this galaxy, which is typically large in PRGs, from  $10^8$  to  $10^{10} M_{\odot}$ , (see Iodice 2014, and references therein). In particular, since the gas is usually associated to the polar structure, the baryonic mass of this component in FCSS J033710.0-354727 could be even higher. Thus, as lower limits for the stellar mass ratio between the central disk and the polar structure we found 3:1 to 2:1.

#### 4. Results: the Ongoing Formation of a Wide Polar Ring/Disk

The deep exposures in the  $g$  and  $i$  bands, combined with the high angular resolution of the OmegaCAM at VST, allow us to carry out the first detailed photometric analysis of the background galaxy FCSS J033710.0-354727 at  $z \sim 0.05$ , in the field of the Fornax cluster.

<sup>3</sup> The radius of each circular aperture is set to include two times the peak of light.

<sup>4</sup> *Galaxies Isochrone Synthesis Spectral Evolution Library*

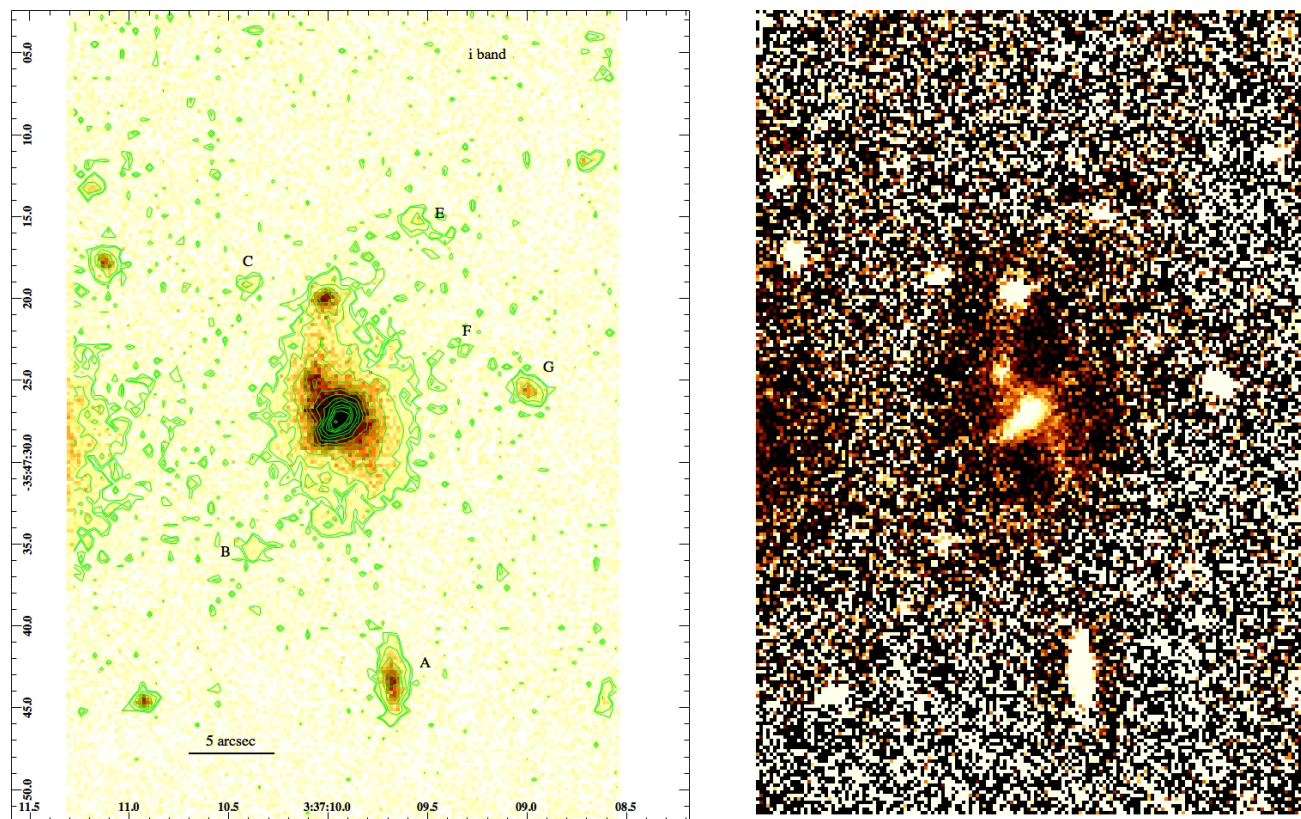


**Fig. 3.** Left panel - VST image of FCSS J033710.0-354727 in *i*-band and the isophote contours (green lines). Labels are the same as in Fig.1 2. Right panel - The *high frequency residual images* of FCSS J033710.0-354727 in the *i*-band. North is up and East is on the left.

**Table 2.** Integrated magnitudes and colors for regions in FCSS J033710.0-354727 in circular apertures.

Region	$\alpha$	$\delta$	R	$m_g$	$m_i$	$g - i$
(1)	[sec]	[arcsec]	[arcsec]	[mag]	[mag]	[mag]
X	09.93	27.15	1.05	$21.14 \pm 0.02$	$20.61 \pm 0.02$	$0.53 \pm 0.04$
Y	10.07	24.71	1.05	$21.98 \pm 0.03$	$21.63 \pm 0.03$	$0.35 \pm 0.06$
Z	09.94	20.17	1.47	$21.64 \pm 0.02$	$21.53 \pm 0.03$	$0.11 \pm 0.05$
A	09.67	43.39	2.31	$22.57 \pm 0.04$	$21.30 \pm 0.02$	$1.27 \pm 0.05$
B	10.38	35.53	1.89	$23.68 \pm 0.07$	$22.65 \pm 0.06$	$1.03 \pm 0.13$
C	10.41	19.29	1.47	$23.95 \pm 0.08$	$23.01 \pm 0.07$	$0.94 \pm 0.15$
D	09.69	11.61	1.89	$23.75 \pm 0.08$	$23.49 \pm 0.12$	$0.26 \pm 0.2$
E	09.55	15.28	1.89	$23.16 \pm 0.06$	$22.48 \pm 0.06$	$0.68 \pm 0.12$
F	09.30	23.13	1.47	$24.00 \pm 0.08$	$23.41 \pm 0.10$	$0.60 \pm 0.2$
G	09.00	24.79	2.31	$23.00 \pm 0.05$	$21.93 \pm 0.04$	$1.07 \pm 0.09$

*Col. 1:* Region of FCSS J033710.0-354727 labelled in Fig. 2. *Col. 2 and Col. 3:* Celestial coordinates of the the center of each circular aperture, see left panel of Fig. 2 for reference. *Col. 4* Radius of the circular aperture in arcsec. *Col. 5 and Col. 6:* Integrated magnitudes in the *g* and *i* bands corrected for the Galactic Extinction. *Col. 7* Integrated  $g - i$  color.

Main results obtained in the present work (see Sec.3) show that:

- the system is characterized by a central component, surrounded by a warped ring-like structure (see Fig. 2 and Fig. 4.);
- the central component is a disk with an exponential surface brightness profile;
- the polar structure is 2 times more extended than the central disk. It crosses the galaxy center, along the North-South direction, drawing a spiral loop throughout the nucleus. It is characterised by two bright knots, one of them (**Z**) having an almost comparable luminosity to that of the galaxy center;

- the central galaxy is redder ( $g - i \sim 0.55$  mag) than the polar structure ( $g - i \sim 0.13 - 0.4$  mag);
- the integrated colors of the bright objects detected around FCSS J033710.0-354727, have a "bimodal" distribution. Only those located on the NW region have ( $g - i$ ) colors comparable with those derived for the polar structure (see Table 2), thus they can be considered as features "related" to the galaxy.

The new observations and analysis are in favor of the classification of this galaxy as PRG. In particular, the whole morphology and the large polar extension suggests that this system can be considered as good candidate for a wide polar ring/disk galaxy,

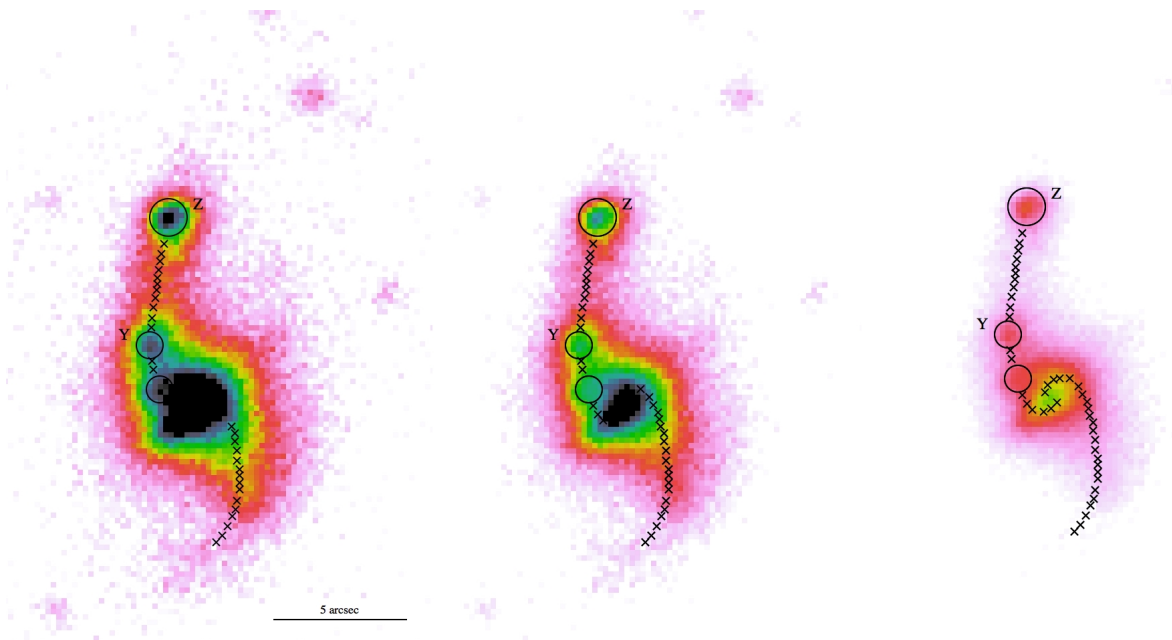


**Fig. 4.** VST images of FCSS J033710.0-354727 in *g*-band with different contrasts in order to emphasize the morphology of the galaxy close to center. The maximum level increases from left to the right. Labels are the same as in Fig.1 2. The three circles indicates the bright blobs of light along the northern arm of the polar structure. The crosses signature in each panel "follows" the bright path of the polar structure up to the galaxy center (see Sec. 3 for details). North is up and East is on the left.

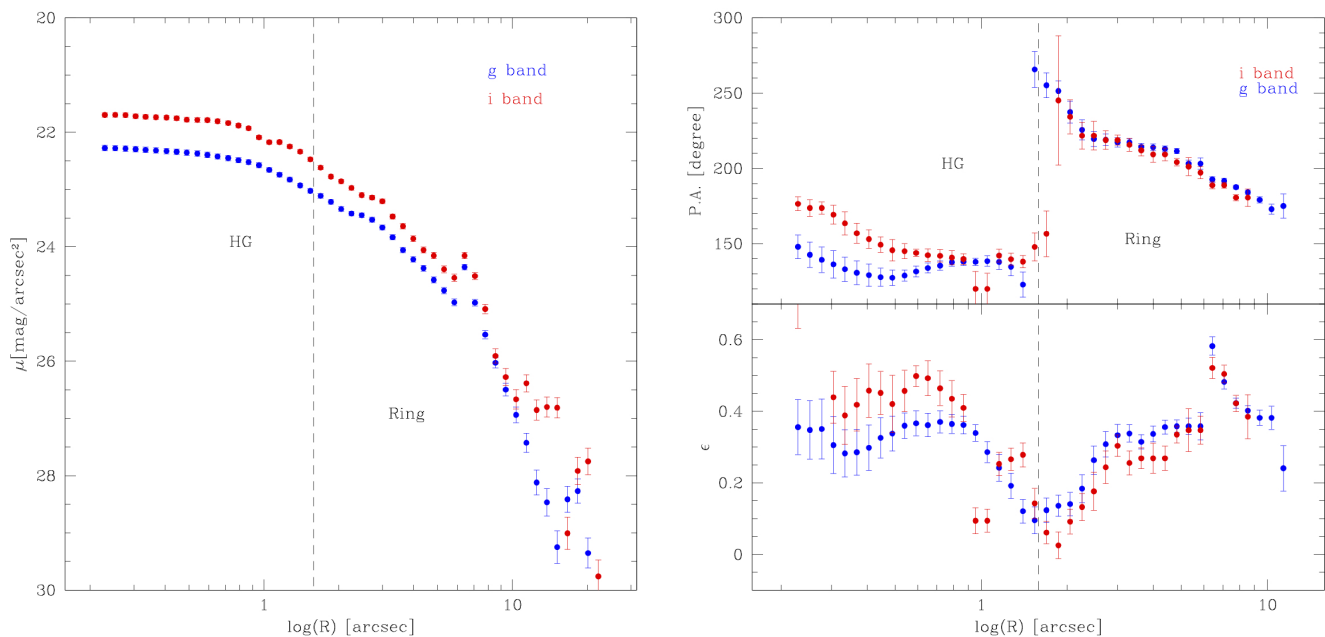


**Fig. 5.** Left panel - Azimuthally averaged surface brightness profiles as function of  $\log(R)$ , derived by the isophote fit.  $R$  is the isophote major axis. Data are for the *g*-band image (blue dots) and *i*-band (red dots). The dashed line delimits the regions where the main components (HG and polar ring) of the galaxy structure are located. Right panel - Average profiles of P.A. (top panel) and ellipticity (bottom panel) as function of  $\log(R)$ .

like NGC 4650A (Iodice et al. 2002). In FCSS J033710.0-354727, the warped geometry of the polar structure and the presence of bright knots along its light distribution, as well as the several debris observed on the NW side with similar colors, suggest that the polar structure is still forming. Given the high luminosity, comparable with that of the galaxy center, the two knots **Y** and **Z** (see Fig. 2) could be the remnant of a companion galaxy that is disrupting in the potential of the central disk,

which is 2-3 times more massive than the accreting object. This mechanism, i.e. the tidal accretion of material from outside, is one of the possible formation scenario proposed for PRGs (see Combes 2014, as review). In this framework, taking into account the small stellar mass ratio between the central disk and the polar structure (3:1 - 2:1), and the high inclination of the accreting material, numerical simulations (Bournaud & Combes 2003) are able to form a massive and extended polar ring/disk as observed

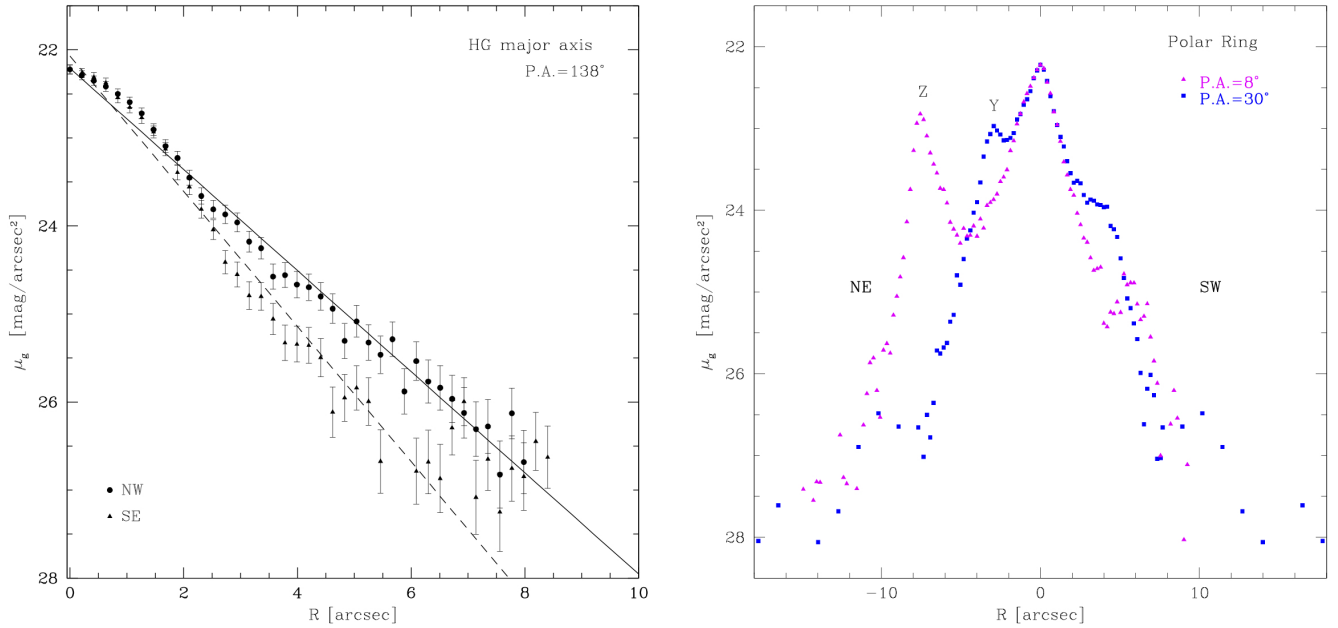


**Fig. 7.** Left panel - Folded light profiles in the  $g$  band along the major axis of the central spheroid. The continuous and dashed lines are the results of the exponential fits to the light distribution for NW (circles) and SE (triangles) sides respectively (see Sec. 3 for details.) Right panel - Light profiles in the  $g$  band along the polar structure. The two directions at  $P.A. = 8^\circ$  and  $P.A. = 30^\circ$  are chosen to intersect the two bright knots **Y** and **Z**, observed on the north arm, respectively (see also Fig. 2 left panel).

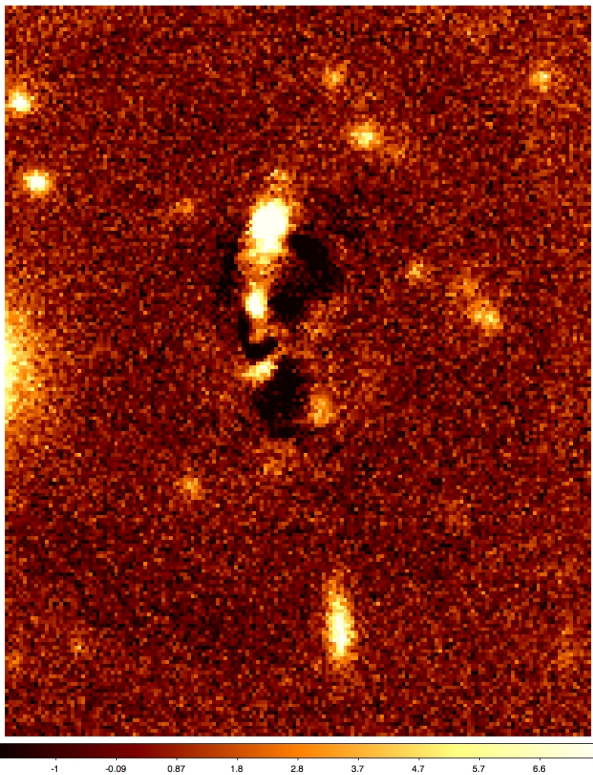


**Fig. 6.** Residual image obtained by subtracting off the 2D model derived from the fit of isophotes to the original image in the  $g$  band. The image size is  $34 \times 42$  arcsec ( $\sim 34 \times 42$  kpc).

in FCSS J033710.0-354727. By comparing the snapshots of the simulation with the observed morphology for FCSS J033710.0-354727, we suggest that this kind of gravitational interaction is

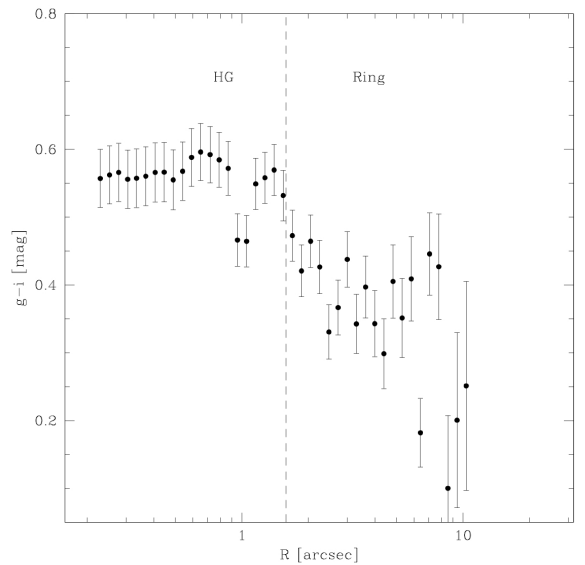


**Fig. 8.** Azimuthally averaged  $g - i$  color profile as function of  $\log(R)$ , derived by the isophote fit.  $R$  is the isophote major axis. The dashed line delimits the regions where the main components (HG and polar ring) of the galaxy structure are located.

still in act, thus we are looking at the intermediate stage of the PRG formation, at the epoch of about 2 Gyr.

Alternatively, FCSS J033710.0-354727 might also be a post-merger system, where two big galaxies have already coalesced into the single system, with two tidal tails around it and an accumulation of mass at the tip of the northern tail. Something like NGC 7252 (Hibbard & Mihos 1995). One observational fact in favour of the tidal accretion process, instead of the major merger,

is the large mass of the the bright knot **Z**, not typically found in tidal tail, and the "S-shape" feature that connects the outer parts of polar structure to the galaxy center (see right panel of Fig. 2), which is more similar to an accreting loop rather than a tidal tail remnants. Kinematic measurements are needed, not only to confirm FCSS J033710.0-354727 as PRG, but also to discriminate between the two formation mechanisms. In particular, if this galaxy is the remnant of a major merger between two disk galaxies we expect to found the central object dominated by random motions (Bournaud & Combes 2003).

In conclusion, FCSS J033710.0-354727 is a peculiar system at  $z \sim 0.05$  resulting from the interaction of two massive galaxies, which could form a wide polar ring/disk galaxy. As discussed in Sec. 1, the few PRGs studied at  $z \geq 0.05$  show a well-formed polar structure, without any tail or ripple that could suggest an ongoing interaction event. The main result of this work is that, up to date, FCSS J033710.0-354727 is the most distant *PRGs in formation* for which a detailed photometric analysis has been performed: the intermediate stage "captured" for this object allows us to derive the important constraint on the mass ratio of the two interacting galaxies, which is hard to estimate, or quite uncertain, in a final remnant galaxy.

*Acknowledgements.* We are very grateful to the anonymous referee for his/her comments and suggestions which helped us to improve and clarify our work. This work was supported by the PRIN-INAF "Galaxy Evolution with the VLT Survey Telescope (VST)" (PI A. Grado). M. Cantiello acknowledges support from PO FSE Abruzzo 2007-2013 (PO 2012/2013).

## References

- Bournaud, F. & Combes, F. 2003, *A&A*, 401, 817  
 Brocca, C., Bettoni, D., & Galletta, G. 1997, *A&A*, 326, 907  
 Brosch, N., Kniazev, A. Y., Moiseev, A., & Pustilnik, S. A. 2010, *MNRAS*, 401, 2067  
 Bruzual, G. & Charlot, S. 2003, *MNRAS*, 344, 1000  
 Capaccioli, M. & Schipani, P. 2011, *The Messenger*, 146, 2  
 Chilingarian, I. V., Melchior, A.-L., & Zolotukhin, I. Y. 2010, *MNRAS*, 405, 1409  
 Chilingarian, I. V. & Zolotukhin, I. Y. 2012, *MNRAS*, 419, 1727  
 Combes, F. 2014, in *Astronomical Society of the Pacific Conference Series*, Vol. 486, *Multi-Spin Galaxies*, ASP Conference Series, ed. E. Iodice & E. M. Corsini, 207  
 Conselice, C. J. 2014, in *Astronomical Society of the Pacific Conference Series*, Vol. 486, *Multi-Spin Galaxies*, ASP Conference Series, ed. E. Iodice & E. M. Corsini, 85  
 Drinkwater, M. J., Phillipps, S., Jones, J. B., et al. 2000, *A&A*, 355, 900  
 Grado, A., Capaccioli, M., Limatola, L., & Getman, F. 2012, *Memorie della Societa Astronomica Italiana Supplementi*, 19, 362  
 Hibbard, J. E. & Mihos, J. C. 1995, *AJ*, 110, 140  
 Iodice, E. 2014, in *Astronomical Society of the Pacific Conference Series*, Vol. 486, *Astronomical Society of the Pacific Conference Series*, ed. E. Iodice & E. M. Corsini, 39  
 Iodice, E., Arnaboldi, M., De Lucia, G., et al. 2002, *AJ*, 123, 195  
 Kuijken, K. 2011, *The Messenger*, 146, 8  
 Moiseev, A. V., Smirnova, K. I., Smirnova, A. A., & Reshetnikov, V. P. 2011, *MNRAS*, 418, 244  
 Reshetnikov, V. P. 1997, *A&A*, 321, 749  
 Reshetnikov, V. P. & Dettmar, R.-J. 2007, *Astronomy Letters*, 33, 222  
 Reshetnikov, V. P., Hagen-Thorn, V. A., & Yakovleva, V. A. 1996, *A&A*, 314, 729  
 Ripepi, V., Cignoni, M., Tosi, M., et al. 2014, *MNRAS*, 442, 1897  
 Schipani, P., D'Orsi, S., Ferragina, L., et al. 2010, *Appl. Opt.*, 49, 1234  
 Schipani, P., Noethe, L., Arcidiacono, C., et al. 2012, *Journal of the Optical Society of America A*, 29, 1359  
 Schlegel, D. J., Finkbeiner, D. P., & Davis, M. 1998, *ApJ*, 500, 525  
 Spavone, M. & Iodice, E. 2013, *mnras*, 434, 3310  
 Spavone, M., Iodice, E., Bettoni, D., et al. 2012, *mnras*, 426, 2003  
 Stanonik, K., Platen, E., Aragón-Calvo, M. A., et al. 2009, *ApJ*, 696, L6